Journal of Medicinal Chemistry

Article

pubs.acs.org/jmc

Rational Design of Orthogonal Multipolar Interactions with Fluorine in Protein−Ligand Complexes

Jonathan Pollock,[†] Dmitry Borkin,[†] George Lund,[†] Trupta Purohit,[†] Edyta Dyguda-Kazimierowicz,[‡] Jolanta Grembecka,[†] and Tomasz Cierpicki*[,†]

[†]Department of Pathology, University of Michigan, Ann Arbor, Michigan 48109, United States

[‡]Molecular Modeling and Quantum Chemistry Group, Department of Chemistry, Wrocław University of Technology, Wyb. Wyspiańskiego 27, 50-370 Wrocław, Poland

Supporting Information

ABSTRACT: Multipolar interactions involving fluorine and the protein backbone have been frequently observed in protein−ligand complexes. Such fluorine−backbone interactions may substantially contribute to the high affinity of small molecule inhibitors. Here we found that introduction of trifluoromethyl groups into two different sites in the thienopyrimidine class of menin−MLL inhibitors considerably improved their inhibitory activity. In both cases, trifluoromethyl groups are engaged in short interactions with the backbone of menin. In order to understand the effect of fluorine, we synthesized a series of analogues by systematically changing the number of fluorine atoms, and we determined high-resolution crystal structures of the complexes with menin. We found that introduction of fluorine at favorable geometry for interactions with backbone carbonyls may improve the activity of menin−MLL inhibitors as much as 5- to 10-fold. In order to facilitate the design of multipolar fluorine−backbone interactions in protein−ligand complexes, we developed a computational algorithm named FMAP, which calculates fluorophilic sites in proximity to the protein backbone. We demonstrated that FMAP could be used to rationalize improvement in the activity of known protein inhibitors upon introduction of fluorine. Furthermore, FMAP may also represent a valuable tool for designing new fluorine substitutions and support ligand optimization in drug discovery projects. Analysis of the menin−MLL inhibitor complexes revealed that the backbone in secondary structures is particularly accessible to the interactions with fluorine. Considering that secondary structure elements are frequently exposed at protein interfaces, we postulate that multipolar fluorine−backbone interactions may represent a particularly attractive approach to improve inhibitors of protein−protein interactions.

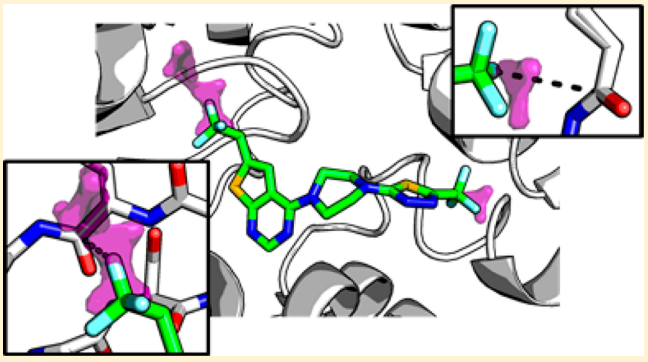

INTRODUCTION

Fluorine has been recognized as a valuable element in medicinal chemistry, and about 20−25% known drugs contain fluorine atoms.[1−3] Fluorine is the most electronegative element and has a strong effect on physicochemical and conformational properties of organic compounds.[3] As a consequence, introduction of fluorine atoms into ligands is a promising strategy in lead optimization to strengthen protein−ligand interactions. Furthermore, introduction of fluorine into ligand molecules affects physicochemical properties and modulates absorption, distribution, metabolism, and excretion in drug-like molecules.[2,3]

Fluorine can enhance ligand affinity through interaction with both polar and hydrophobic groups in proteins.[4] While organic fluorine is a very poor hydrogen bond acceptor,[5] interaction of C−F with polar hydrogen atoms has been observed in protein−inhibitor complexes.[1,6,7] An interesting mode of fluorine interactions has been observed for thrombin inhibitors where substitution of hydrogen with fluorine resulted in 5-fold increase in potency.[8] The crystal structure revealed that fluorine is in remarkably close (3.1 Å) contact to the carbonyl moiety of Asn98. Further analysis of the Cambridge Structural Database (CSD) and Protein Data Bank (PDB) showed that short F···C═O contacts (3.0−3.7 Å) are abundant in both organic compounds and protein−ligand complexes, and the fluorine atom frequently approaches the electrophilic carbonyl carbon atom in an orthogonal arrangement.[2,4,8,9] For example, in the trifluoroacetyl dipeptide anilide inhibitor bound to elastase (PDB code 2EST), all three fluorines are involved in close contacts with backbone carbonyl groups. Orthogonal multipolar C−F···C═O interactions have been observed with both backbone as well side chain carbonyls, and several studies have recognized these interactions as an attractive approach to increase ligand binding affinity.[2,9,10]

Previous studies have demonstrated that very potent inhibitors can be developed through the use of fluorine substitutions. For example, a low nanomolar inhibitor of dipeptidyl peptidase IV has been developed by the introduction of several fluorine atoms.[7] Introduction of trifluoromethyl groups during the

Received: June 23, 2015
Published: August 19, 2015

DOI: 10.1021/acs.jmedchem.5b00975
J. Med. Chem. 2015, 58, 7465−7474

optimization of fragment-derived ligands resulted in the development of picomolar inhibitors of Cytochrome bc1 Complex.[11] Fluorine scanning has been proposed as an effective strategy for ligand optimization.[8,10] Systematic incorporation of fluorine at different positions in a series of thrombin inhibitors revealed that introduction of fluorine into the benzyl ring enhanced the binding affinity by 6-fold.[8] As a step toward the identification of fluorophilic hot-spots in proteins, it has been proposed to use ^{19}F NMR ligand-based screening of fluorinated fragments[12] and a combination of screening and computational analysis.[13] However, a rational approach for designing fluorinated ligands is missing.

We previously identified the thienopyrimidine class of compounds which directly bind to menin and inhibit the protein−protein interaction (PPI) between menin and MLL with nanomolar affinity.[14] Substitution of a propyl group on the thienopyrimidine scaffold with trifluoroethyl, which resulted in the MI-2-2 compound, leads to a significant 10-fold increase in the binding affinity.[15] The crystal structure of MI-2-2 bound to menin revealed that the CF_3 group is involved in close contacts with the protein backbone. This demonstrates that fluorine−backbone interactions offer excellent opportunities to enhance the activity of inhibitors targeting protein−protein interactions. However, introduction of fluorine atoms into ligand molecules might be synthetically challenging or may require multistep synthesis. Therefore, a method for rational design of favorable fluorine interactions in protein−ligand complexes would significantly facilitate inhibitor development in drug discovery projects. In order to understand the effect of fluorine substitutions, we synthesized series of MI-2-2 analogues systematically changing the number of fluorine atoms in two different groups and determined high-resolution crystal structures of the inhibitors bound to menin. We found that when fluorine atoms in menin inhibitors are involved in the orthogonal multipolar C−F···C═O interactions, it significantly enhances ligand binding affinity. On the basis of these findings, we developed a computational algorithm named FMAP to support structure-based design of favorable C−F···C═O interactions in protein−ligand complexes, and we demonstrated its applicability to known fluorine-containing small molecule inhibitors. This study should facilitate rational development of fluorinated ligands for drug discovery applications.

MATERIALS AND METHODS

PDB Search of Fluorine Containing Protein−Ligand Complexes. We performed a search of the PDB to identify protein−ligand complexes containing fluorine atoms. We identified 2559 crystal structures containing a fluorinated ligand and performed an analysis using a python script to select structures in which a fluorine atom is located within 3.5 Å of either the peptide backbone carbonyl carbon or amide nitrogen. We have accepted structures with 2.2 Å resolution or better for further analysis. We found a total of 442 protein−ligand complexes, which fit these criteria for detailed analysis.

FMAP Fluorine Site Mapping Algorithm and Filtering Criteria. FMAP calculates favorable positions for fluorine to form C−F···C═O interactions with the protein backbone. Geometrical criteria are selected to cover ∼80% of the fluorine positions identified in the small molecule ligands observed in our PDB search. Calculation of the fluorine sites is initiated by defining an arbitrary number of 29 hypothetical fluorine sites within 3 Å distance from either the backbone carbon or nitrogen (Table S1). Subsequently, FMAP uses a series of filters to remove fluorine positions using following criteria: (1) steric clash; fluorines within 1.8 Å of any protein atom are removed. (2) entirely buried or overly exposed fluorines; this filter removes positions that are not accessible to small molecules or are entirely exposed, such as protein termini, loops; this is accomplished through a summation the number of Cαs closer than 10 Å and the number of total atoms closer than 5 Å; any position with a Cα count between 15 and 28 and a total atom count less than 30 is retained. (3) fluorines too close to carbonyl oxygens; positions are eliminated when closer than 2.7 Å from a carbonyl oxygen and less than 60 degrees off the C═O bond vector, eliminating positions that are too close to the electron lone pairs of carbonyl oxygens. (4) isolated sites; this procedure eliminates isolated fluorines, removing positions that are not clustered with other nearby fluorines; fluorines with less than 5 adjacent fluorines within 3.2 Å are removed.

FMAP is written in python, and can be run either as a pymol extension or as a standalone command-line program. Results of FMAP calculations are displayed in Pymol using surface representation that encompasses a volume of 2.8−3.2 Å distance from the protein backbone. FMAP is freely available from the authors upon request and requires the Biopython module.[16,17]

Calculation of Interaction Energy. Theoretical evaluation of the fluorine interaction energy within model complexes was performed with a fluoromethane probe positioned against the peptide bond present in a model compound. As a model of peptide bond we used *N*-acetylglycine-*N*-methylamide in extended conformation. Geometrical parameters to mapping the interaction energy were defined by setting the origin of the spherical coordinate system onto the position of the carbon atom from the peptide bond carbonyl group. Radial distances as well as polar and azimuthal angles were then varied by 0.1 Å and 10 degrees, respectively. Within the C···F distance range of 2.5−4.0 Å, all the combinations of polar and azimuthal angles were considered except for those resulting in steric clashes. Fluoromethane orientation was optimized at the HF/6-31+G(d) level of theory with model peptide and fluorine atoms kept frozen. The resulting structures were used for MP2/6-31G(d) interaction energy calculation. Counterpoise correction was applied to reduce the basis set superposition error.[18] We selected MP2/6-31G(d) level of theory because it provides appropriate estimation of binding energy in biomolecular complexes.[19] All the quantum chemical calculations were performed using the Gaussian09 program.[20]

Expression and Purification of Menin. Full-length human menin was expressed in a pET32a vector (Promega) containing N-terminal thioredoxin His_6-tag in Rosetta (DE3) cells. Menin was purified using nickel-agarose (GE Healthcare) followed by ion exchange with Q-Sepharose (GE Healthcare). Protein was subsequently cleaved with thrombin followed by nickel agarose purification to separate the thioredoxine tag from menin. Purified protein was dialyzed to 50 mM Tris, 50 mM NaCl, 1 mM TCEP pH 7.5 buffer. Details of menin purification have been published previously.[21]

Chemistry. The synthesis and characterization of menin−MLL inhibitor is presented in (see Supporting Information).

Characterization of Activity of Menin−MLL Inhibitors. Activity of small molecules to inhibit the menin−MLL interaction was determined by fluorescence polarization (FP) assay. This assay used FITC-MBM1 peptide of MLL (residues 4−15) at 15 nM with 150 nM menin in 50 mM Tris, 50 mM NaCl, 1 mM DTT pH 7.5 buffer. The detailed protocol has been described previously.[21] The IC_{50} values represent mean values

DOI: 10.1021/acs.jmedchem.5b00975
J. Med. Chem. 2015, 58, 7465−7474

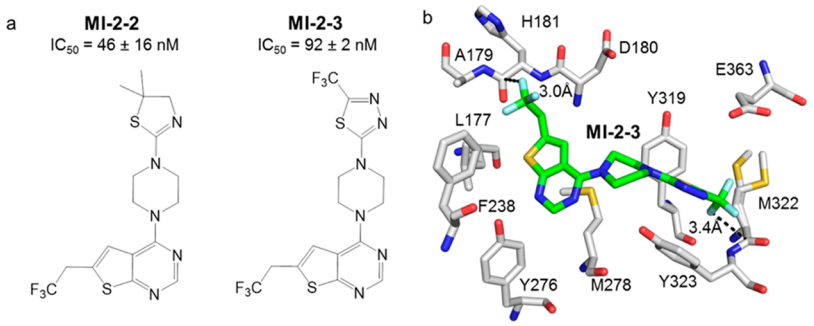

Figure 1. Inhibitors of the menin−MLL interaction containing CF_3 groups. (a) Structures and activities of MI-2-2 and MI-2-3. (b) Crystal structure of MI-2-3 bound to menin. Short C−F···C═O distances are shown using dashed lines.

and standard deviations from two to three independent experiments.

Crystallization of the Menin Complexes with Small Molecule Inhibitors. Co-crystallization of menin with small molecule inhibitors was performed with 2.5 mg/mL menin[15] incubated with 3-fold molar excess small-molecule inhibitors (MI-326, MI-333, MI-319, MI-2-3, MI-836, MI-859, or MI-273). Crystals were obtained using a sitting-drop technique at 10 °C in 0.2 M ammonium acetate, 0.1 M HEPES, pH 7.5, and 25% w/v PEG 3350. Prior to data collection, crystals were transferred to cryosolution containing 20% PEG550 MME and flash-frozen in liquid nitrogen as described previously.[15]

Crystallographic Data Collection and Structure Determination. X-ray diffraction data for cocrystals of menin with small molecule inhibitors were collected at 21-ID-D, 21-ID-F, and 21-ID-G beamlines at the Life Sciences Collaborative Access Team at the Advanced Photon Source. Data was processed with HKL-2000.[22] Structures of the complexes were determined by molecular replacement using MOLREP with the apo structure of human menin (PDB code: 4GPQ) as a search model. The model was refined using REFMAC,[23] COOT,[24] and the CCP4 package.[25] In the final stages, refinement was performed with addition of the TLS groups defined by the TLSMD server.[26] Validation of the structures was performed using MOLPROBITY[27] and ADIT.[28] Details of data processing and refinement are summarized in Table S2. Coordinates and structure factors have been deposited in the Protein Data Bank.

RESULTS AND DISCUSSION

Trifluoromethyl Groups in Menin−MLL Inhibitors Form Close Contacts with Protein Backbone. We previously performed extensive medicinal chemistry optimization of the thienopyrimidine class of menin−MLL inhibitors and found that substitution of propyl in the MI-2 compound by trifluoroethyl group resulted in a substantial, 10-fold increase in the activity of MI-2-2 (Figure 1a and Table S3).[15] Due to difficulties for further substitutions and potential metabolic liability of the thiazoline moiety, we modified this class of compounds by replacing thiazoline with an aromatic thiadiazole ring. Although the unsubstituted thiadiazole analogue is very weak,[14] we found that introduction of the trifluoromethyl group substantially improved the activity, resulting in MI-2-3 with IC_{50} = 92 nM (Figure 1a). Both compounds, MI-2-2 and MI-2-3, are potent inhibitors of the menin−MLL interaction with the IC_{50} values below 100 nM (Figure 1a). Our previous studies revealed that one fluorine atom from the trifluoroethyl group in MI-2-2 forms close contacts with the backbone atoms on menin and is located within 3.0 Å distance to the backbone carbonyl of His181,[15] suggesting that this interaction might play an important role in increasing the inhibitory activity of MI-2-2 over MI-2. To understand the molecular basis of high binding affinity of MI-2-3, we determined the crystal structure of its complex with menin. The newly developed MI-2-3 with an additional trifluoromethyl group binds to menin in a similar binding mode as MI-2-2 (Figure 1b). Interestingly, the new CF_3 group within the trifluoromethyl−thiadiazole moiety also forms close contacts with the menin backbone (Figure 1b), and one of the fluorine atoms is located 3.4 Å from the carbonyl group of Met322. Therefore, the fluorine atoms in both CF_3 groups of MI-2-3 are involved in orthogonal multipolar C−F···C═O interactions with the backbone atoms in two different regions on menin. To assess the contribution of the CF_3 group in MI-2-3, we synthesized MI-326 by replacing trifluoromethyl with the methyl group and found that it led to ∼8-fold decrease in the inhibitory activity (IC_{50} = 779 nM for MI-326, Table S3). These two examples, MI-2-2 and MI-2-3, emphasize that C−F···C═O contribute very favorably to the protein−ligand interactions.[2,8,10]

Development of FMAP Algorithm To Predict Multipolar C−F···C═O Interactions. Multipolar interactions involving fluorine atoms have been recognized for their pronounced effect on protein−ligand interactions, and well-placed fluorine may substantially enhance the activity of small molecule inhibitors.[2,8−10] Introduction of trifluoromethyl groups in menin inhibitors resulted in a significant improvement of inhibitory activity due to formation of short-distance multipolar interactions with the protein backbone. We therefore sought whether such interactions could be rationally designed. First, we analyzed the geometry of fluorine−backbone interactions in known high-resolution crystal structures of protein−ligand complexes (see Methods). Out of 2559 structures containing fluorinated ligands, we found 442 complexes with a fluorine atom within 3.5 Å of either the backbone carbonyl carbon or amide nitrogen. This search demonstrated that fluorine is frequently located within a short distance of the backbone carbonyl group with the C−F bond preferrably oriented in the orthogonal arrangement relative to the plane of the peptide bond (Figure 2a). This exemplifies a presence of multipolar C−F···C═O interactions as described in detail in the previous studies.[2,9] We have also performed theoretical calculations of the interaction energy between the model peptide bond and fluoromethane. We found favorable interaction energy for the C−F positioned above the peptide carbonyl group, which is consistent with the analysis of experimental structures (Figure 2b).

On the basis of the analysis of protein−ligand complexes from the Protein Data Bank (PDB), we developed an algorithm (FMAP) for mapping sites for fluorine atoms on protein structures to form

DOI: 10.1021/acs.jmedchem.5b00975
J. Med. Chem. 2015, 58, 7465−7474

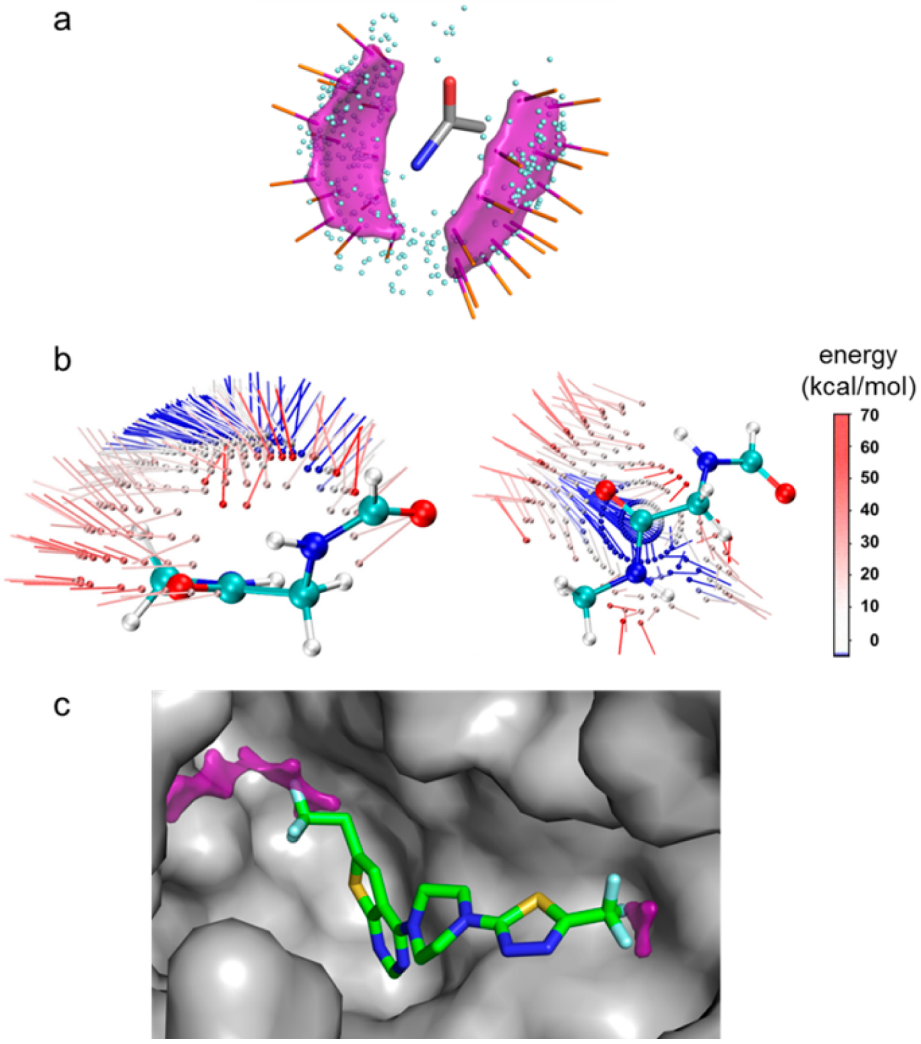

Figure 2. Prediction of favorable C−F···C═O interactions using FMAP algorithm. (a) Combined analysis of protein−ligand structures from PDB, with FMAP predictions of the potential fluorine positions and their representative C−F bonds relative to backbone peptide bond. Positions of fluorine atoms derived from the protein−ligand complexes found in PDB are shown as cyan points. FMAP prediction is shown as purple surface with orange vectors shown for representative C−F bonds. (b) Binding energy calculations (kcal/mol) for interaction of fluoromethane with a model peptide using MP2/6-31G(d) theory level as a function of C−F bond orientation. Distance between fluorine and carbonyl carbon is set to 3 Å. Fluorines are represented as small balls, and the C−F bonds are represented as sticks. Model peptide is presented in balls and sticks representation (carbon in cyan, oxygen in red, and nitrogen in blue). (c) FMAP prediction for the menin-MI-2-3 complex. Purple surface represents favorable positions for fluorine atoms to interact with protein backbone.

favorable C−F···C═O interactions with the protein backbone. The geometric criteria used in FMAP have been selected to encompass ∼80% of fluorine sites found in the experimental structures in PDB. Fluorine sites are mapped onto a protein structure through a Pymol[29] extension and are represented as a surface spanning 2.8−3.2 Å range from the peptide bond (Figure 2a). FMAP also eliminates unlikely fluorine positions through filters based on unfavorable geometry for multipolar interactions as well as steric clashes with protein atoms (see Methods for a detailed description of FMAP).

We employed FMAP to analyze the inhibitor binding site on menin and found that there are two potential sites for accessing close contacts between fluorine and protein backbone. Importantly, both sites are occupied by the CF_3 groups in the complex of menin with MI-2-3 (Figure 2c), supporting the utility of FMAP for the prediction of fluorophilic sites in protein structures. The first site is relatively small and is occupied by the CF_3 group connected to the thiadiazole moiety, whereas the second site is much larger and is occupied by the trifluoroethyl group attached to the thienopyrimidine scaffold. Close inspection of the menin-MI-2-3 crystal structure revealed that only a single fluorine in each CF_3 group has favorable geometry for C−F···C═O interactions with backbone. On the basis of this analysis, we concluded that most likely not all fluorines are needed for high-affinity interactions of menin with the MI-2-3 and MI-2-2 inhibitors.

Interactions of Trifluoromethyl−Thiadiazole Moiety with Menin. FMAP analysis suggested that only one fluorine atom in the CF_3 group within the trifluoromethyl-thiadiazole moiety of MI-2-3 is capable of favorable interactions with the backbone carbonyl of Met332. In order to evaluate the contributions of fluorine atoms to the binding affinity of MI-2-3, we synthesized a series of analogues replacing CF_3 with CH_3, CH_2F, and CHF_2 groups (Figure 3). First, we assessed the effect of substituting CF_3 by CH_3 and found that the absence of the three fluorine atoms in MI-326 results in >8 fold decrease in the

DOI: 10.1021/acs.jmedchem.5b00975
J. Med. Chem. 2015, 58, 7465−7474

a

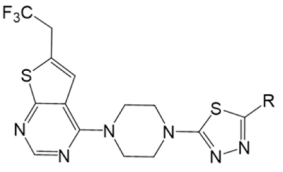

	R	IC_{50} (nM)	ΔΔG (kcal/mol)
MI-326	CH_3	779 ± 27	0
MI-333	CH_2F	1653 ± 332	0.44
MI-319	CHF_2	82 ± 9	-1.3
MI-2-3	CF_3	92 ± 2	-1.2

b

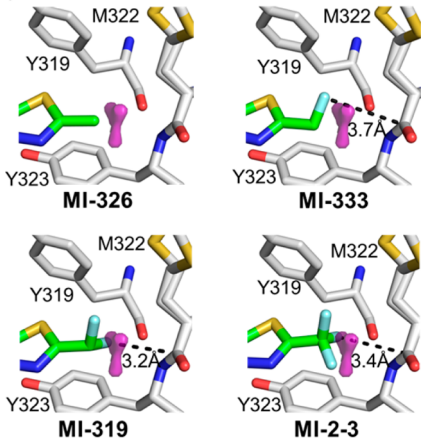

Figure 3. Effect of fluorine substitutions in thiadiazole moiety on activity of menin−MLL inhibitors. (a) Structures and activities of inhibitors. ΔΔ*G* values are calculated relative to MI-326. (b) Crystal structures of inhibitors bound to menin showing the shortest distances between fluorine and menin backbone. FMAP prediction is shown as purple surface.

inhibitory activity (Figure 3a). The crystal structure revealed that MI-326 binds to menin in a very similar manner as MI-2-3 (Figure 3b), and the difference in the binding affinity predominantly results from the loss of the fluorine atoms. We then synthesized and tested two additional analogues with two (MI-319) and single (MI-333) fluorines. The inhibitory activity of MI-319 is very similar to MI-2-3 indicating no differences between CF_3 and CHF_2 groups (Figure 3a). Surprisingly, MI-333, which harbors the CH_2F group, has about 20-fold weaker activity than MI-2-3 and is even 2-fold less potent than MI-326 with no fluorines (Figure 3a). To explain this effect, we determined the crystal structures of MI-333 and MI-319 bound to menin. The CHF_2 group in MI-319 binds in a very similar manner as CF_3 with one of the fluorine atoms in a short, 3.2 Å, distance to the backbone carbonyl of Met322 (Figure 3b). On the contrary, the single fluorine in MI-333 adopts a position that is tilted approximately 38.5° from the plane of the thiadiazole ring and points away from the protein backbone (3.7 Å distance to C═O of Met322) (Figure 3b). As a consequence, the fluorine is too far to be involved in a favorable multipolar C−F···C═O interactions, and no gain in the activity is observed for MI-333 (Figure 3a).

The orientation of the CH_2F group relative to the thiadiazole ring was unexpected, emphasizing a strong conformational effect of the fluorine atom. As previously observed, substitution of H by F can profoundly change the conformational preferences of a small molecule because of the size and stereoelectronic effects.[2] Although we were able to predict the position of fluorine required for favorable interactions with the protein backbone using FMAP, we did not anticipate that CH_2F can adopt an orientation where the fluorine points away from the backbone. Introduction of the second fluorine into the CHF_2 group was necessary to achieve an orientation of the C−F bond allowing for favorable C−F···C═O interactions and substantial improvement in activity. Analysis of the crystal structure of MI-333 shows that S−C−C−F dihedral adapts 38.5° angle. Quantum mechanical energy calculations of rotational energy barrier for CFH_2 group in MI-333 shows two minima at −55 and 55°, and the conformation in the crystal structure is disfavored by about 0.5 kcal/mol (Figure S1). On the contrary, in MI-319, one fluorine is positioned in the energetical minimum (S−C−C−F dihedral angle equal to −49°) while the second fluorine which has less favorable geometry (S−C−C−F dihedral angle equal to 71°) can interact with backbone. This example demonstrates that while only single fluorine may interact with backbone, other fluorines might be needed to stabilize the appropriate rotameric state.

Interactions of Trifluoroethyl Group in Thienopyrimidine Core with Menin. Comparison of the activities of MI-2-2 and MI-19 indicates that the trifluoroethyl group contributes significantly to the high activity of MI-2-2, and replacement of CF_3 with CH_3 results in over 20-fold loss in inhibitory activity (Figure 4a). FMAP analysis for the menin binding site suggests that only single fluorine in CF_3 group can form C−F···C═O interactions with the backbone. To test the contributions of individual fluorines in the CF_3 group of MI-2-2, we synthesized two compounds with CH_2F (MI-836) or CHF_2 (MI-859) groups. When compared to MI-19, addition of the first fluorine enhanced the activity nearly 5-fold, whereas addition of the second fluorine increased the activity further by about 4-fold, making it comparable to MI-2-2 with CF_3 group (Figure 4a). To rationalize the effect of these modifications, we determined the crystal structures of MI-836 and MI-859 bound to menin (Figure 4b). We found that the single fluorine in MI-836 points toward a hydrophobic site formed by the side chains of Leu177, Phe238, Ala182, and Ser155, and therefore, the 5-fold gain in the activity likely results from favorable hydrophobic contacts. Introduction of CHF_2 in MI-859 allows for the second fluorine to be involved in the C−F···C═O interactions with the backbone of His181, accounting for an additional 4-fold improvement in activity.

Very similar IC_{50} values of MI-859 (with CHF_2) and MI-2-2 (with CF_3) indicates that the third fluorine is dispensable for binding. Furthermore, the cLogP value for MI-859 is approximately 0.6 unit lower than for MI-2-2 (cLogP = 3.89 and 3.32 for MI-2-2 and MI-859, respectively). Therefore, our approach based on the FMAP calculations may be used not only to predict fluorine substitutions in ligand molecules but also to design compounds with fewer number of fluorine atoms and reduced lipophilicity without compromising ligand binding affinity.

Analysis of the MI-2-2-menin structure revealed that the methylene group in the CH_2CF_3 moiety is positioned closely to the backbone carbonyl groups of Ser178 and Glu179 and may constitute a further site for fluorine substitutions. However, the FMAP analysis revealed that introduction of the CF_2 group at this site would not be favorable due to poor geometry of the two fluorines with respect to the carbonyl groups of Ser178 and Glu179. To test this hypothesis, we synthesized MI-273 with CF_2CF_3 group and found that such a substitution results in a ∼15-fold decrease in the activity when compared to MI-2-2 (Figure 4a). We determined the crystal structure of MI-273 bound to menin and found that it binds in an identical manner as

DOI: 10.1021/acs.jmedchem.5b00975
J. Med. Chem. 2015, 58, 7465−7474

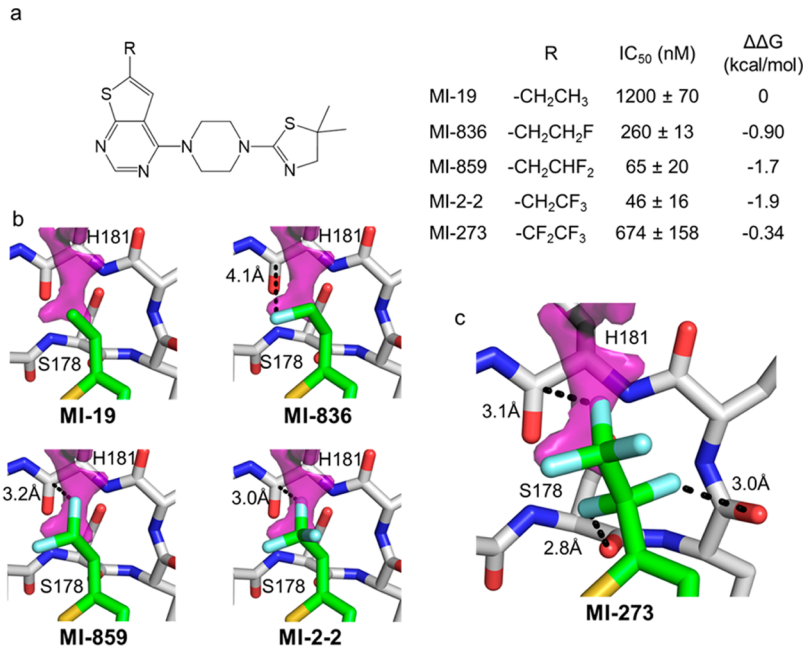

Figure 4. Effect of fluorine substitutions in thienopyrimidine moiety on activity of menin−MLL inhibitors. (a) Structures and activities of inhibitors. $\Delta\Delta G$ values are calculated relative to MI-19. (b) Crystal structures of inhibitors bound to menin showing the shortest distances between fluorine and the menin backbone. FMAP prediction is shown as purple surface. Model of MI-19 has been made on the basis of the structure of MI-2-2-menin complex. (c) Crystal structure of MI-273 bound to menin showing close contacts of fluorines in CF_2CF_3 group with menin. FMAP prediction is shown as purple surface.

MI-2-2 (Figure 4c). The two additional fluorines in the CF_2 group of MI-273 are in close distances to the carbonyl oxygens of Ser178 and Glu179 leading to repulsive interactions. This further emphasizes that favorable C−F···C═O interactions require optimal geometry, and the FMAP approach can filter-out the sites that are unfavorable for fluorine atoms in ligand molecules.

Application of FMAP To Rationalize Fluorine Substitutions in Known Ligands. One of the first well-documented examples of the C−F···C═O interactions favorably contributing to protein−ligand interaction was described for the tricyclic class of thrombin inhibitors.[8] The 4-fluoro substitution of benzyl group in compound **1** resulted in over 5-fold improvement in inhibitory activity for **2**. Analysis of the crystal structure of **2** bound to thrombin revealed short distance between fluorine and backbone carbonyl of Asn98.[8] We performed FMAP analysis of this complex and found that fluorine in **2** fits well into the FMAP predicted site for the C−F···C═O interactions (Figure 5a). Therefore, FMAP could be a valuable tool to predict 4-fluoro substitution in **1** to increase its potency.

We also found several other examples of ligands for which the activity of unsubstituted and fluorine substituted analogues have been determined and the crystal structures of fluorine analogues bound to the target proteins are available. In a recent example, potent inhibitors of procaspace-6 have been developed using a fragment-based discovery approach.[30] Substitution of the phenyl ring in **3** with a fluorine resulting in compound **4** led to a 6-fold improvement in the binding affinity. The crystal structure demonstrated that fluorine in **4** is in a close, 3.1 to 3.2 Å, distance from the carbonyl groups of Ala195 and Ser196 and is involved in favorable C−F···C═O interactions (Figure 5b). Again, the position of fluorine in **4** is consistent with the FMAP prediction (Figure 5b). Structure-based design of HIV-1 entry inhibitors resulted in development of tetramethylpiperidine class of compounds, which bind to the viral envelope glycoprotein gp120.[31] Introduction of fluorine into the phenyl ring in **5** yielded 5-fold more potent inhibitor **6**, and structural analysis of a very close analogue of **6** revealed that fluorine is within the 3.5 Å distance to the carbonyl group of Ser256, which overlaps well with the FMAP prediction for favorable positions of fluorine in the binding sites (Figure 5c). Another interesting example of the C−F···C═O interactions has been observed for the β-lactamase inhibitor. Introduction of the CF_3 group into phenyl ring of **7** resulted in a large, 24-fold increase in the affinity for **8** (Figure 5d).[32] Although substitution of hydrogen by trifluoromethyl group represents a relatively large structural perturbation, the CF_3-group in the crystal structure of **8** bound to β-lactamase is mostly solvent exposed, and one of the fluorines is located within a short, 3.2 Å distance to the carbonyl of Thr319, which fits well into the FMAP prediction (Figure 5d).

We have recently exploited the idea to introduce C−F···C═O interactions into the hydroxymethylpiperidine class of the menin−MLL inhibitors.[33] Structure analysis revealed that this class of inhibitors binds to the same pocket on menin as thienopyrimidine compounds and that the phenyl ring overlaps with the position of trifluoroethyl in MI-2-2.[33] We synthesized analogue **10** with the 3-fluorophenyl group to introduce fluorine pointing toward the carbonyl group of His181 and found that this leads to 2-fold improvement in the inhibitory activity (Figure 5e). FMAP analysis predicted favorable fluorine substitution at this position and the crystal structure of **10** bound to menin validated that fluorine indeed participates in the C−F···C═O interactions (Figure 5e). Introduction of the aromatic fluorine atom into the hydroxymethylpiperidine class of menin−MLL inhibitors has a less pronounced effect than in the thienopyrimidine class likely due to the slightly longer distance between fluorine and the carbonyl of His181 (3.2 vs 3.0 Å, respectively) and less favorable geometry. Interestingly, addition of fluorine into this site also resulted in a significant improvement in the affinity of the macrocyclic peptidomimetic inhibitor of the menin−MLL interaction.[34] A compound with fluorine at

DOI: 10.1021/acs.jmedchem.5b00975
J. Med. Chem. 2015, 58, 7465−7474

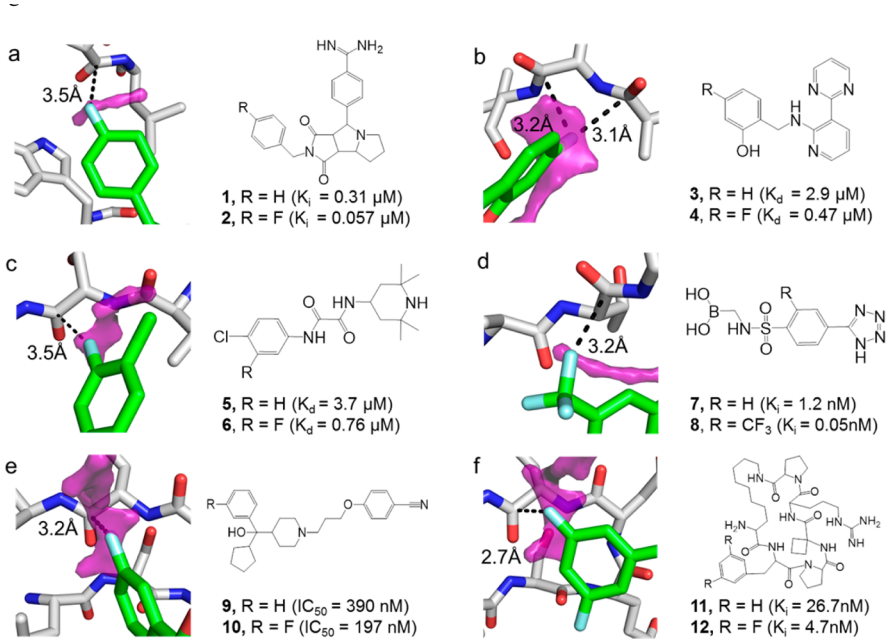

Figure 5. Analysis of FMAP calculations for known inhibitors containing fluorine atoms. Crystal structure of protein−inhibitor complexes showing close C−F···C═O contacts and FMAP predictions (in purple). The structures of inhibitors and activities are also reported. (a) thrombin inhibitor (PDB code 1OYT). (b) procaspase-6 inhibitor (PDB code 4NBL). (c) gp120 inhibitor (PDB code 4DKO). (d) β-lactamase inhibitor (PDB code 4E3N). (e) menin−MLL inhibitor (PDB code 4OG6). (f) macrocyclic menin−MLL inhibitor (model based on PDB structure 4I80).

the meta position of the phenyl ring has 4-fold better binding affinity when compared with the unsubstituted analogue.[34] We modeled the meta-fluoro analogue using the crystal structure of menin with the macrocyclic peptidomimetic inhibitor and found that fluorine is expected to occupy the site that remains in a short distance to the carbonyl of His181 and overlaps well with the FMAP predictions (Figure 5f).

We have also found examples where substitution with fluorine did not have beneficial effect on inhibitory activity despite reasonably good agreement with the FMAP predictions. In two such examples, introduction of fluorine into inhibitors of neuronal nitric oxide synthase and c-Jun N-terminal kinase 1 led to the modest decrease in the inhibitory activity (Figure S2).[35,36] This indicates that prediction of fluorine substitutions based solely on geometrical criteria might have potential limitations, and other factors such as effect of fluorine on stereoelectronic or conformational properties of the ligand, structural changes upon ligand binding, might need to be considered in order to further improve the design of C−F···C═O interactions.

Designing C−F···C═O Interactions at PPI Interfaces. Targeting protein−protein interactions (PPIs) using small molecule inhibitors is considered challenging, and the most "druggable" PPIs belong to the protein-peptide class of complexes.[37−39] Interfaces at such PPIs frequently feature secondary structure elements such as α-helical bundle[40] or addition of β-sheet.[41] Development of potent small molecule inhibitors targeting such PPI interfaces could significantly benefit from optimization of the inhibitor-backbone contacts. Interestingly, analysis of the menin MI-2-3 structure reveals that the two CF_3 groups form similar C−F···C═O contacts but with the two structurally different backbone conformations. The CF_3 group at the thiadiazole interacts with α-helix, whereas the CF_3 attached to the thienopyrimidine core interacts with β-sheet on menin (Figure 6a,c).

We have used FMAP to analyze accessibility of protein backbone in the secondary structure elements to participate in

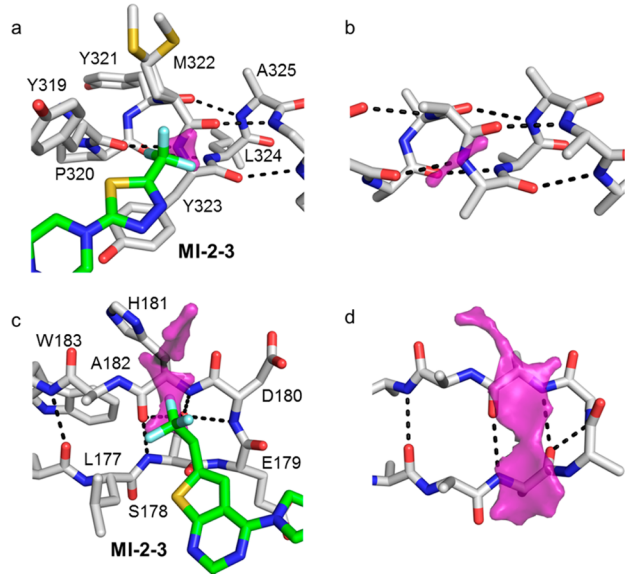

Figure 6. FMAP predictions for α-helix and β-sheet structures. (a) Details of the interaction of CF_3 group in MI-2-3 with α-helical fragment in menin and FMAP prediction. (b) FMAP prediction for idealized α-helix for a single peptide bond. Orientation of the α-helix is similar as in panel a. (c) Details of the interaction of CF_3 group in MI-2-3 with β-sheet in menin. (d) FMAP prediction for idealized β-sheet structure shown in similar orientation as in panel c.

the C−F···C═O interactions. We performed the FMAP calculations for idealized secondary structures composed of the poly-Ala sequences and found that only a small area of the α-helix is accessible to interact with fluorine, whereas a much larger surface area could interact with fluorine in β-sheet or β-hairpin (Figure 6). The access to protein backbone in α−helical conformation is small and restricted via amino acid side chains (Figure 6b). Therefore, there is limited access of the fluorine to the peptide

DOI: 10.1021/acs.jmedchem.5b00975
J. Med. Chem. 2015, 58, 7465−7474

bond in order to participate in the orthogonal C−F···C═O interactions. On the contrary, the access to peptide bonds in β-sheet conformation is significantly larger, and fluorine may be positioned over a relatively large area to favorably interact with the backbone (Figure 6d), facilitating the design of fluorinated ligands. This analysis clearly indicates a potential to design favorable interactions involving fluorine in ligands that bind at PPI interfaces. Design of such interactions should be particularly feasible for interfaces involving β-sheets due to the relatively large accessibility of protein backbone.

CONCLUSIONS

Fluorine scanning strategy has been previously proposed as an effective approach to improve the activity of small molecule inhibitors.[2,8,10] Such a strategy is synthetically demanding and requires synthesis of multiple analogues.[8,10] In an attempt to facilitate design of C−F···C═O interactions in protein−ligand complexes we developed the FMAP algorithm. FMAP uses a crystal structure of a protein−ligand complex and calculates sites surrounding a ligand which could be favorably occupied by fluorine atoms. We demonstrated that FMAP could be used to rationalize improvement in activity upon introduction of fluorine in thienopyrimidine class of menin inhibitors as well as for several known inhibitors. FMAP may also represent a valuable tool for the design of new fluorine substitutions in protein ligands. FMAP relies solely on geometrical and structural criteria, and other effects, such as conformational or electronic changes resulting from fluorine substitution are not taken into account, which might represent a limitation of this approach. Nevertheless, we expect that FMAP can be very useful in the drug discovery projects to rationally design positions for flourine atoms in ligand molecules. It may also support development of ligands with an optimal number of fluorine atoms to improve binding affinity while reducing ligand hydrophobicity and molecular weight.

Introduction of the CF_3 group in menin inhibitors as well as in several examples reviewed in this study results in a substantial gain in the affinity providing that optimal geometry of the C−F bond relative to the backbone carbonyl is achieved. Such C−F···C═O interactions provide unique opportunities to introduce favorable interactions between small molecule ligands and the polar protein backbone. Due to unique orthogonal geometry relative to the protein backbone, these interactions may be introduced into the binding sites where hydrogen bonds are not feasible. We found that substitution of CH_3 for CF_3 may increase ligand binding affinity as much as 10-fold. However, multipolar interactions involving the CF_3 group may not be solely responsible for the increase in binding affinity. The effect of desolvatation of more hydrophobic CF_3 group is expected to lead to a larger positive entropy of binding when compared with CH_3.[42] The CF_3 is roughly twice the size of a methyl group[1] and due to a larger size and different shape, it may form more optimal van der Waals contacts within the binding site. Furthermore, the two additional fluorine atoms may participate in hydrophobic interactions with neighboring atoms. In the case of menin inhibitors, we found that not all fluorine atoms in the CF_3 group are needed for the high affinity interaction. However, introduction of CFH_2 or CF_2H groups to achieve favorable C−F···C═O interactions may impact conformational equilibrium and favor a rotamer which cannot favorably interact with protein backbone or might cause high entropic cost of freezing out a desired rotamer. Despite that the H to F substitution represents a relatively minor modification, it may have a complex impact on ligand binding affinity. Our structural data collected for the menin−inhibitor complexes offers a unique set of data which may facilitate better understanding of the C−F···C═O interactions.

The C−F···C═O interactions have been typically reported for enzyme inhibitors.[8,10,30,32] With increasing interest and demand in development of PPI inhibitors, efficient approaches are needed to optimize protein−ligand interactions at solvent exposed interfaces. As we demonstrated for the menin−MLL inhibitors, fluorine interaction with the protein backbone may offer such opportunities, particularly at the interfaces involving α-helical or β-sheet structures. In this study, we developed the FMAP approach to streamline the design of C−F···C═O interactions, which adds a new tool for structure-based design of new inhibitors targeting protein−protein interfaces as well as protein ligands in a more general context. The FMAP algorithm may facilitate prediction of fluorine substitutions in ligand molecules and support ligand optimization in drug discovery projects.

ASSOCIATED CONTENT

Supporting Information

The Supporting Information is available free of charge on the ACS Publications website at DOI: 10.1021/acs.jmedchem.5b00975.

Supplemental data and methods for synthesis and characterization (PDF)
Compound data (CSV)

AUTHOR INFORMATION

Corresponding Author

*E-mail: tomaszc@umich.edu. Tel: 734-615-9324.

Notes

The authors declare the following competing financial interest(s): Drs. Grembecka and Cierpicki receive research support from Kura Oncology. They are also receiving compensation as members of the scientific advisory board of Kura Oncology, and they have an equity ownership in the company. Other coauthors declare no potential conflict of interest.

ACKNOWLEDGMENTS

This work was supported by the American Cancer Society grants (RSG-11-082-01-DMC to T.C. and RSG-13-130-01-CDD to J.G.), NIH R01 CA181185 to T.C., NIH R01 CA160467 to J.G., Leukemia and Lymphoma Society (LLS) TRP grant (6116-12) to J.G., LLS Scholar (1215-14) to J.G. Use of the Advanced Photon Source, an Office of Science User Facility operated for the U.S. Department of Energy (DOE) Office of Science by Argonne National Laboratory, was supported by the U.S. DOE under Contract No. DE-AC02-06CH11357. Use of the LS-CAT Sector 21 was supported by the Michigan Economic Development Corporation and the Michigan Technology Tri-Corridor (Grant 085P1000817).

REFERENCES

(1) Bohm, H. J.; Banner, D.; Bendels, S.; Kansy, M.; Kuhn, B.; Muller, K.; Obst-Sander, U.; Stahl, M. Fluorine in medicinal chemistry. *ChemBioChem* **2004**, *5*, 637−43.
(2) Muller, K.; Faeh, C.; Diederich, F. Fluorine in pharmaceuticals: looking beyond intuition. *Science* **2007**, *317*, 1881−6.
(3) Purser, S.; Moore, P. R.; Swallow, S.; Gouverneur, V. Fluorine in medicinal chemistry. *Chem. Soc. Rev.* **2008**, *37*, 320−30.
(4) Bissantz, C.; Kuhn, B.; Stahl, M. A medicinal chemist's guide to molecular interactions. *J. Med. Chem.* **2010**, *53*, 5061−84.
(5) Dunitz, J. D.; Taylor, R. Organic fluorine hardly ever accepts hydrogen bonds. *Chem. - Eur. J.* **1997**, *3*, 89−98.

DOI: 10.1021/acs.jmedchem.5b00975
J. Med. Chem. 2015, 58, 7465−7474

(6) Parlow, J. J.; Kurumbail, R. G.; Stegeman, R. A.; Stevens, A. M.; Stallings, W. C.; South, M. S. Design, synthesis, and crystal structure of selective 2-pyridone tissue factor VIIa inhibitors. *J. Med. Chem.* **2003**, *46*, 4696−701.
(7) Kim, D.; Wang, L.; Beconi, M.; Eiermann, G. J.; Fisher, M. H.; He, H.; Hickey, G. J.; Kowalchick, J. E.; Leiting, B.; Lyons, K.; Marsilio, F.; McCann, M. E.; Patel, R. A.; Petrov, A.; Scapin, G.; Patel, S. B.; Roy, R. S.; Wu, J. K.; Wyvratt, M. J.; Zhang, B. B.; Zhu, L.; Thornberry, N. A.; Weber, A. E. (2R)-4-oxo-4-[3-(trifluoromethyl)-5,6-dihydro[1,2,4]-triazolo[4,3-a]pyrazin-7(8H)- yl]-1-(2,4,5-trifluorophenyl)butan-2-amine: a potent, orally active dipeptidyl peptidase IV inhibitor for the treatment of type 2 diabetes. *J. Med. Chem.* **2005**, *48*, 141−51.
(8) Olsen, J. A.; Banner, D. W.; Seiler, P.; Sander, U. O.; D'Arcy, A.; Stihle, M.; Muller, K.; Diederich, F. A fluorine scan of thrombin inhibitors to map the fluorophilicity/fluorophobicity of an enzyme active site: Evidence for C-F center dot center dot center dot C═O interactions. *Angew. Chem., Int. Ed.* **2003**, *42*, 2507−2511.
(9) Paulini, R.; Muller, K.; Diederich, F. Orthogonal multipolar interactions in structural chemistry and biology. *Angew. Chem., Int. Ed.* **2005**, *44*, 1788−1805.
(10) Olsen, J. A.; Banner, D. W.; Seiler, P.; Wagner, B.; Tschopp, T.; Obst-Sander, U.; Kansy, M.; Muller, K.; Diederich, F. Fluorine interactions at the thrombin active site: protein backbone fragments H-C(alpha)-C═O comprise a favorable C-F environment and interactions of C-F with electrophiles. *ChemBioChem* **2004**, *5*, 666−75.
(11) Hao, G. F.; Wang, F.; Li, H.; Zhu, X. L.; Yang, W. C.; Huang, L. S.; Wu, J. W.; Berry, E. A.; Yang, G. F. Computational discovery of picomolar Q(o) site inhibitors of cytochrome bc1 complex. *J. Am. Chem. Soc.* **2012**, *134*, 11168−76.
(12) Vulpetti, A.; Hommel, U.; Landrum, G.; Lewis, R.; Dalvit, C. Design and NMR-based screening of LEF, a library of chemical fragments with different local environment of fluorine. *J. Am. Chem. Soc.* **2009**, *131*, 12949−59.
(13) Vulpetti, A.; Schiering, N.; Dalvit, C. Combined use of computational chemistry, NMR screening, and X-ray crystallography for identification and characterization of fluorophilic protein environments. *Proteins: Struct., Funct., Genet.* **2010**, *78*, 3281−91.
(14) Grembecka, J.; He, S.; Shi, A.; Purohit, T.; Muntean, A. G.; Sorenson, R. J.; Showalter, H. D.; Murai, M. J.; Belcher, A. M.; Hartley, T.; Hess, J. L.; Cierpicki, T. Menin-MLL inhibitors reverse oncogenic activity of MLL fusion proteins in leukemia. *Nat. Chem. Biol.* **2012**, *8*, 277−84.
(15) Shi, A.; Murai, M. J.; He, S.; Lund, G.; Hartley, T.; Purohit, T.; Reddy, G.; Chruszcz, M.; Grembecka, J.; Cierpicki, T. Structural insights into inhibition of the bivalent menin-MLL interaction by small molecules in leukemia. *Blood* **2012**, *120*, 4461−9.
(16) Hamelryck, T.; Manderick, B. PDB file parser and structure class implemented in Python. *Bioinformatics* **2003**, *19*, 2308−10.
(17) Cock, P. J.; Antao, T.; Chang, J. T.; Chapman, B. A.; Cox, C. J.; Dalke, A.; Friedberg, I.; Hamelryck, T.; Kauff, F.; Wilczynski, B.; de Hoon, M. J. Biopython: freely available Python tools for computational molecular biology and bioinformatics. *Bioinformatics* **2009**, *25*, 1422−3.
(18) Boys, S.; Bernardi, F. The calculation of small molecular interactions by the differences of separate total energies. Some procedures with reduced errors. *Mol. Phys.* **1970**, *19*, 553−566.
(19) Giedroyc-Piasecka, W.; Dyguda-Kazimierowicz, E.; Beker, W.; Mor, M.; Lodola, A.; Sokalski, W. A. Physical Nature of Fatty Acid Amide Hydrolase Interactions with Its Inhibitors: Testing a Simple Nonempirical Scoring Model. *J. Phys. Chem. B* **2014**, *118*, 14727−14736.
(20) Frisch, M. J.; Trucks, G. W.; Schlegel, H. B.; Scuseria, G. E.; Robb, M. A.; Cheeseman, J. R.; Scalmani, G.; Barone, V.; Mennucci, B.; Petersson, G. A.; Nakatsuji, H.; Caricato, M.; Li, X.; Hratchian, H. P.; Izmaylov, A. F.; Bloino, J.; Zheng, G.; Sonnenberg, J. L.; Hada, M.; Ehara, M.; Toyota, K.; Fukuda, R.; Hasegawa, J.; Ishida, M.; Nakajima, T.; Honda, Y.; Kitao, O.; Nakai, H.; Vreven, T.; Montgomery Jr., J. A.; Peralta, J. E.; Ogliaro, F.; Bearpark, M. J.; Heyd, J.; Brothers, E. N.; Kudin, K. N.; Staroverov, V. N.; Kobayashi, R.; Normand, J.; Raghavachari, K.; Rendell, A. P.; Burant, J. C.; Iyengar, S. S.; Tomasi, J.; Cossi, M.; Rega, N.; Millam, N. J.; Klene, M.; Knox, J. E.; Cross, J. B.; Bakken, V.; Adamo, C.; Jaramillo, J.; Gomperts, R.; Stratmann, R. E.; Yazyev, O.; Austin, A. J.; Cammi, R.; Pomelli, C.; Ochterski, J. W.; Martin, R. L.; Morokuma, K.; Zakrzewski, V. G.; Voth, G. A.; Salvador, P.; Dannenberg, J. J.; Dapprich, S.; Daniels, A. D.; Farkas, Ö.; Foresman, J. B.; Ortiz, J. V.; Cioslowski, J.; Fox, D. J. *Gaussian 09*; Gaussian, Inc.: Wallingford, CT, 2009.
(21) Grembecka, J.; Belcher, A. M.; Hartley, T.; Cierpicki, T. Molecular basis of the mixed lineage leukemia-menin interaction: implications for targeting mixed lineage leukemias. *J. Biol. Chem.* **2010**, *285*, 40690−8.
(22) Otwinowski, Z.; Minor, W. Processing of X-ray diffraction data collected in oscillation mode. *Methods Enzymol.* **1997**, *276*, 307−326.
(23) Murshudov, G. N.; Vagin, A. A.; Dodson, E. J. Refinement of macromolecular structures by the maximum-likelihood method. *Acta Crystallogr., Sect. D: Biol. Crystallogr.* **1997**, *53*, 240−55.
(24) Emsley, P.; Cowtan, K. Coot: model-building tools for molecular graphics. *Acta Crystallogr., Sect. D: Biol. Crystallogr.* **2004**, *60*, 2126−32.
(25) Collaborative Computational Project, N. The CCP4 suite: programs for protein crystallography. *Acta Crystallogr., Sect. D: Biol. Crystallogr.* **1994**, *50*, 760−763.10.1107/S0907444994003112.
(26) Painter, J.; Merritt, E. A. TLSMD web server for the generation of multi-group TLS models. *J. Appl. Crystallogr.* **2006**, *39*, 109−111.
(27) Davis, I. W.; Leaver-Fay, A.; Chen, V. B.; Block, J. N.; Kapral, G. J.; Wang, X.; Murray, L. W.; Arendall, W. B., 3rd; Snoeyink, J.; Richardson, J. S.; Richardson, D. C. MolProbity: all-atom contacts and structure validation for proteins and nucleic acids. *Nucleic Acids Res.* **2007**, *35*, W375−83.
(28) Yang, H.; Guranovic, V.; Dutta, S.; Feng, Z.; Berman, H. M.; Westbrook, J. D. Automated and accurate deposition of structures solved by X-ray diffraction to the Protein Data Bank. *Acta Crystallogr., Sect. D: Biol. Crystallogr.* **2004**, *60*, 1833−9.
(29) *The PyMOL Molecular Graphics System*, Version 1.2r3pre, Schrödinger, LLC.
(30) Murray, J.; Giannetti, A. M.; Steffek, M.; Gibbons, P.; Hearn, B. R.; Cohen, F.; Tam, C.; Pozniak, C.; Bravo, B.; Lewcock, J.; Jaishankar, P.; Ly, C. Q.; Zhao, X.; Tang, Y.; Chugha, P.; Arkin, M. R.; Flygare, J.; Renslo, A. R. Tailoring small molecules for an allosteric site on procaspase-6. *ChemMedChem* **2014**, *9* (73−7), 2.
(31) LaLonde, J. M.; Kwon, Y. D.; Jones, D. M.; Sun, A. W.; Courter, J. R.; Soeta, T.; Kobayashi, T.; Princiotto, A. M.; Wu, X.; Schon, A.; Freire, E.; Kwong, P. D.; Mascola, J. R.; Sodroski, J.; Madani, N.; Smith, A. B., 3rd Structure-based design, synthesis, and characterization of dual hotspot small-molecule HIV-1 entry inhibitors. *J. Med. Chem.* **2012**, *55*, 4382−96.
(32) Eidam, O.; Romagnoli, C.; Dalmasso, G.; Barelier, S.; Caselli, E.; Bonnet, R.; Shoichet, B. K.; Prati, F. Fragment-guided design of subnanomolar beta-lactamase inhibitors active in vivo. *Proc. Natl. Acad. Sci. U. S. A.* **2012**, *109*, 17448−53.
(33) He, S.; Senter, T. J.; Pollock, J.; Han, C.; Upadhyay, S. K.; Purohit, T.; Gogliotti, R. D.; Lindsley, C. W.; Cierpicki, T.; Stauffer, S. R.; Grembecka, J. High-affinity small-molecule inhibitors of the menin-mixed lineage leukemia (MLL) interaction closely mimic a natural protein-protein interaction. *J. Med. Chem.* **2014**, *57*, 1543−56.
(34) Zhou, H.; Liu, L.; Huang, J.; Bernard, D.; Karatas, H.; Navarro, A.; Lei, M.; Wang, S. Structure-based design of high-affinity macrocyclic peptidomimetics to block the menin-mixed lineage leukemia 1 (MLL1) protein-protein interaction. *J. Med. Chem.* **2013**, *56*, 1113−23.
(35) Li, B.; Cociorva, O. M.; Nomanbhoy, T.; Weissig, H.; Li, Q.; Nakamura, K.; Liyanage, M.; Zhang, M. C.; Shih, A. Y.; Aban, A.; Hu, Y.; Cajica, J.; Pham, L.; Kozarich, J. W.; Shreder, K. R. Hit-to-lead optimization and kinase selectivity of imidazo[1,2-a]quinoxalin-4-amine derived JNK1 inhibitors. *Bioorg. Med. Chem. Lett.* **2013**, *23*, 5217−22.
(36) Xue, F.; Li, H.; Delker, S. L.; Fang, J.; Martasek, P.; Roman, L. J.; Poulos, T. L.; Silverman, R. B. Potent, highly selective, and orally bioavailable gem-difluorinated monocationic inhibitors of neuronal nitric oxide synthase. *J. Am. Chem. Soc.* **2010**, *132*, 14229−38.
(37) Petsalaki, E.; Russell, R. B. Peptide-mediated interactions in biological systems: new discoveries and applications. *Curr. Opin. Biotechnol.* **2008**, *19*, 344−50.

DOI: 10.1021/acs.jmedchem.5b00975
J. Med. Chem. 2015, 58, 7465−7474

(38) Smith, M. C.; Gestwicki, J. E. Features of protein-protein interactions that translate into potent inhibitors: topology, surface area and affinity. *Expert Rev. Mol. Med.* **2012**, *14*, e16.
(39) Cierpicki, T.; Grembecka, J. Targeting protein-protein interactions in hematologic malignancies: still a challenge or a great opportunity for future therapies? *Immunol Rev.* **2015**, *263*, 279−301.
(40) Jochim, A. L.; Arora, P. S. Assessment of helical interfaces in protein-protein interactions. *Mol. BioSyst.* **2009**, *5*, 924−6.
(41) Remaut, H.; Waksman, G. Protein-protein interaction through beta-strand addition. *Trends Biochem. Sci.* **2006**, *31*, 436−44.
(42) Biffinger, J. C.; Kim, H. W.; DiMagno, S. G. The polar hydrophobicity of fluorinated compounds. *ChemBioChem* **2004**, *5*, 622−7.

DOI: 10.1021/acs.jmedchem.5b00975
J. Med. Chem. 2015, 58, 7465−7474